Journal of Engineering and Applied Sciences 13 (24): 10313-10322, 2018
ISSN: 1816-949X

Preparation, Characterization Nanoparticles Silver Oxide by Electrochemical Method in Different Electrolytic Media and Using as Catalysts

[1]Hayder Khudhair Khattar, [2]Fouad Abdul Ameer Al-Saady and [1]Amer Mousa Jouda
[1]Faculty of Science, University of Kufa, Kufa, Iraq
[2]College of Pharmacy, Al-Mustansiriyah University, Baghdad, Iraq

Abstract: Ag_2O was prepared using a simple chemical technique, a low-cost, easy to use electrodeposition method capable of controlling the size and shape of prepared nanoparticles compared to other methods and using surfactants such as (Glycerin (GLY), Polyvinyl Alcohol (PVA), Poly (N-vinylpyrrolidone) (PVP)) that help the growth and nucleation of suspended particles. The silver oxide is measured by using several techniques such as (Atomic Force Microscopy (AFM), X-Ray Diffraction (XRD), Field Emission Scanning Electron Microscopy (FESEM), Energy-Dispersive X-ray Spectroscopy (EDS) and High Resolution Transmission Electron Microscope (HRTEM). The powder obtained is about 40 nm in order to demonstrate the capacity of the silver oxide as a catalyst calcination at 300°C and standard silver oxide from the Swiss-Fluka company, result indicated an efficiency of up to 91.34, 89.68 PDE% photo degradation energy for silver oxide standard and prepared respectively, parameters influence such as: Energy activation (Ea), Enthalpy of activation (ΔH^0), entropy of activation (ΔS^0) and free energy of activation (ΔG^0) and pH of dye sol and temperature were detailed study. The product photocatalytic reactions suggested that of model are first order pseudo-reactions given by Langmuir-Hinshelwood, the activation energy is equal to 6.950 and 5.804 kJ/mol^{-1} silver oxide standard and prepared, respectively.

Key words: Surfactants, Energy activation (Ea), Enthalpy, XRD, EDS, PVP

INTRODUCTION

The systems associated to nanomaterials, dealing with particles size within the area of 1-100 nm (Schoonman, 2000). The applications of these particles are growing swiftly in numerous domains, such as the bioscience, catalytic, electronic, optics and food manufacture (Ito *et al*., 2005; Yoshida and Toshima, 2014). simple chemical method (Yong *et al*., 2013) and electrochemical method (Fang *et al*., 2012), electrochemistry little advantageous for fabricate dispersions of particles, the insolate products of an electron transport reaction normally precipitates above surface of inert cathode for easy manner electrochemical manner that allows the size and shape was controlled by organization of scattered Ag_2O colloid partials. These Ag_2O flake were produced having a silver electrode as a sacrificing anode to produce a controlled sours of silver ions (Murray *et al*., 2005). The electrochemical technicality are perfectly useful because they give particles with a height purification using quick and simple procedures and controlling the particle size without Difficult by regulate the current density, through the particular technicality particles are acquired with decided size and shape of numerous compositions, in extension, this process is environmental friendly because it harmful reducer agents usually avoid use. Different stabilizers can be utilized in electrochemical techniques, electrostatic stabilizers come with organic monomers and steric stabilizers come from polymeric compounds (Liao *et al*., 2000).

MATERIALS AND METHODS

Experimental work: Electrochemical mode for generating nanoparticles control the size and shape through controlling the current density, voltage and additives for electrolyte nanoparticles. This approach includes using two electrodes, Anode plate made of silver with high purity reaches to 99.99% with scale (1 cm width×3 cm length×1.5 mm thick) and Cathode from graphite with dimensions (2×3 cm×4 mm). The two electrodes are placed facing each other in a vertical way with a distance (2 cm) between each other, the setup is placed in to electrical cell that contains 100 mL Deionized Water (DW) obtained from (Faculty of Pharmacy, University of Kufa, Iraq). The silver particles precipitate on the cathode during the electrolysis, the electrolysis has been employed with the

Corresponding Author: Hayder Khudhair Khattar, Faculty of Science, University of Kufa, Kufa, Iraq

temperatures 60°C with continuous various voltages 15 V, a power supply (DC current, Maximum voltage 30 V, 5 A, China), the current passed in the circuit has been monitored with a voltmeter. Additionally, the electrical circuit has been controlled to change Polarity between the electrodes according the determined period of 5 min. The production of nanoparticles in a way of electrochemical reduction in changing the polarity of the direct current between the electrodes during electrolysis process in order to obtund the better precipitation (Raposo *et al*., 2007).

RESULTS AND DISCUSSION

Characterization of Ag_2O

AFM measurement of Ag_2O powder electro deposition: The AFM analysis of precipitated Ag_2O powder shows in Table 1, the average diameter of Ag_2O with PVA>PVP> glycerin in Fig. 1-3 that the root mean square roughness (sq) is 3.29 nm , i.e., the surface roughness of Ag_2O with stabilizer PVP Which has packs with more heights than other sample with deferent stabilizer such as PVA and glycerin, Srface skewness (Ssk) can be seen negative which means that the surface has more valleys than peaks. The above three specimen have a surface kurtosis (sku) of <3, i.e., that the three sample have a flat surface, The three models in Table 1 are all <3 except sample with PVA is closest to the 3 means that the models are platykurtic (Gadelmawla *et al*., 2002).

X-ray measurements of Ag_2O nanopwoder electrodeposition: X-ray data in the nanopwoder Ag_2O were tested using x-ray diffraction, it come from using a Shimadzu 6000 with Cu Kα radiation (λ = 1.5406 Å) (at 50

Table 1: Conditions and materials used in the experiment of Ag_2O powder electrodeposition of Na_2SO_4 solutions (99% Fluka Analytical , Swiss), Glycerin (GLY), Polyvinyl Alcohol (PVA), Poly (n-vinylpyrrolidone) (PVP) (CDH-India)

----------Chemicals----------		PVP	PVA	Glycerin
Na_2SO_4	0.1 g/100 (mL)	0.1 g/100 (mL)	0.1 g/100 (mL)	0.1 g/100 (mL)
NaOH	5 g/100 (mL)	PH = 12	PH = 12	PH = 12
Deionized water	0.7 (µsec/cm)	0.7 (µsec/cm)	0.7 (µsec/cm)	0.7 (µsec/cm)
Glycerin	(1 g/100 mL)	-	-	10 (mL)
PVA	(1 g/100 mL)	-	10 (mL)	-
PVP	(1 g/100 mL)	10 (mL)	-.	-
Temperature	50-60°C	50-60°C	50-60°C	50-60°C
General currentdensity	500 (A/m^2)	500 (A/m^2)	500 (A/m^2)	500 (A/m^2)
(Silver) Anode area	6 (cm^2)	6 (cm^2)	6 (cm^2)	6 (cm^2)
current density	0.3 (A)	0.3 (A)	0.3 (A)	0.3 (A)
Voltage-time	(V)/(min)	13.8 (V)/155 (min)	15.6 (V)/155 (min)	12.2 (V)/155 (min)

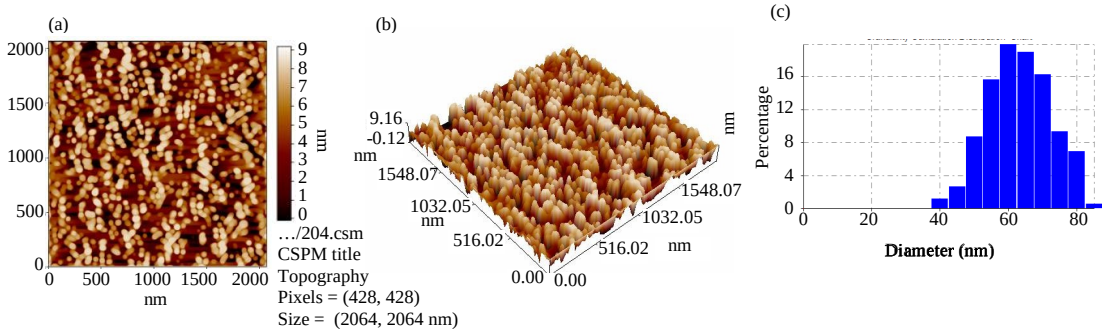

Fig. 1: AFM images of Ag_2O powder electrodeposition of Na_2SO_4 solutions with Glycerin 10 mL. Avg. diameter: 60.87 nm; a) 2-dimensional image; b) 3-dimensinal image and c) Granulite accumulation distribution chart

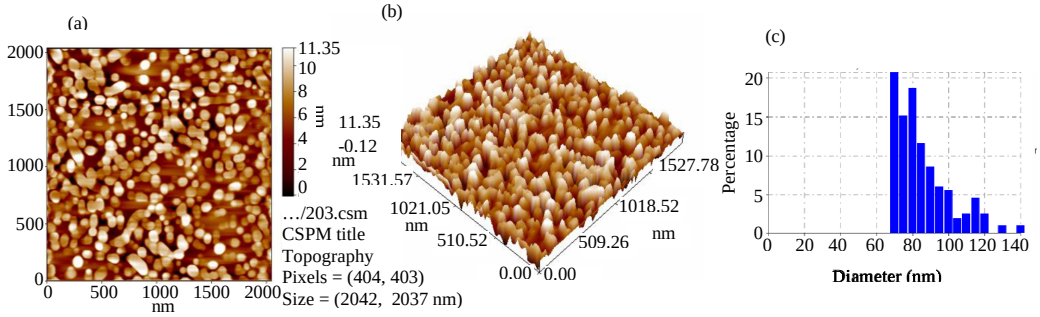

Fig. 2: AFM images of Ag_2O powder electrodeposition of Na_2SO_4 solutions with PVA 10 mL. Avg. diameter: 83.04 nm; a) 2-dimensional image; b) 3-dimensinal image and c) Granulite accumulation distribution chart

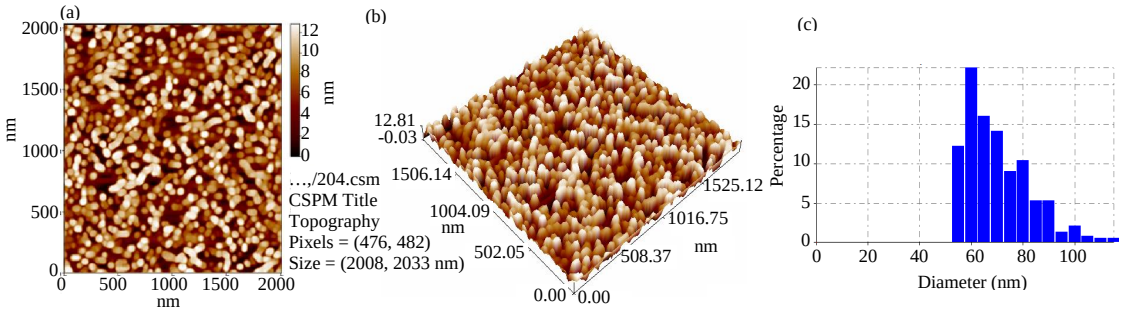

Fig. 3: AFM images of Ag_2O powder electrodeposition of Na2SO4 solutions with PVP 10 mL. Avg. diameter: 67.65 nm; a) 2-dimensional image; b) 3-dimensinal image and c) Granulite accumulation distribution chart

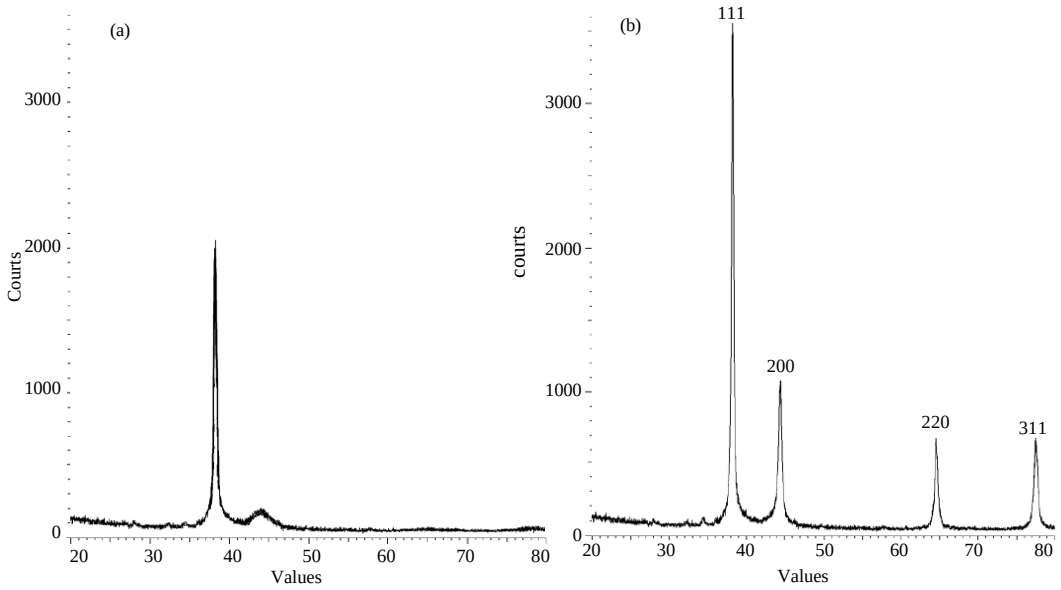

Fig. 4: a)X-ray images of Ag_2O nanopowder amorphous phase and b) Crectallynty phase at 300°C, electro deposition of Na_2SO_4 solutions, Ag_2O particles include (Ag+) with detect {111} faces were explain to be more active at photocatalytic reactions than the particles containing {100} faces (Lyu *et al*., 2010; Ho and Huang, 2009; Kuo and Huang, 2008)

KV and 40 mA) in a scan range (2θ) from 20- 80°, XRD patterns of the as-prepared samples with different conditions were shown in Fig. 4 four sharp peaks can be show at 38.2°, 44.48°, 64.68° and 77.68 to its original indicators (111), (200), (220) and (311), respectively, indicating that the plan (111) of Ag_2O tended to be preferentially oriented within the trial method. All peaks reflected in this mode were found to match the stage of Ag_2O possessing a center cube face (JCPDS: 042-0783) (Privett *et al*., 2010; Rahman *et al*., 2014). The average size of your nano-crystalline (D) was calculated utilize the Debye-Scherrer formula to be about 46 nm.

SEM, TEM and EDS measurements of Ag_2O (NPs) electrodeposition in presence of GLY, PVP, PVA: (FESEM) (Field Emission Scanning Electron Microscopy MIRA3 is a high-resolution, TESCAN, Czech), depending on the working conditions of the constant temperature 60°C and the current, voltage control, the use of stabilizers to improve the reaction speed, get the nucleus and the growth of nanoparticles where the results Inside the nanoscale, the smallest volume of nanoparticles is 20 nm of glycerin, 40 nm of PVP and 60 nm of PVA, TEM (High resolution transmission electron microscope, the Philips CM300 , 300 kV) shown in Fig. 5, the particles are nearly spherical shapes with well-defined boundaries. It is evident from the micrographs that the average size of the particles as directly measured the image is ~20-60 nm, this result's corresponding to obtained from XRD analysis (Sagadevan, 2016) (Fig. 6 and 7).

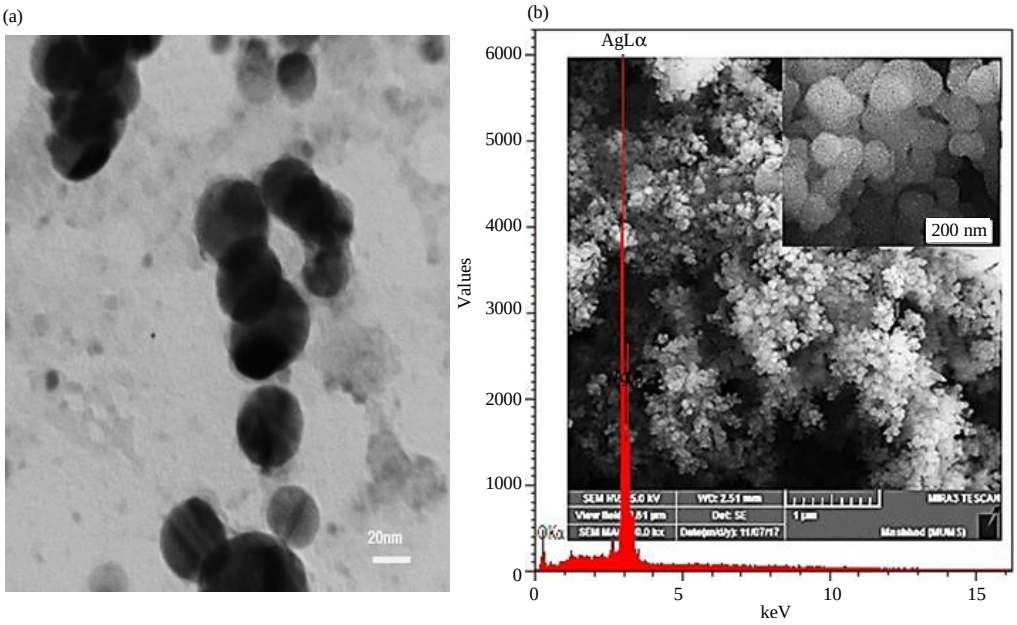

Fig. 5: SEM, TEM and EDS, images of Ag_2O NPs electrodeposition in Na_2SO_4 with GLY 10 mL, 20 nm, vigorous stirring, (Ag = 92.72 wt.%, O = 7.28 wt.%)

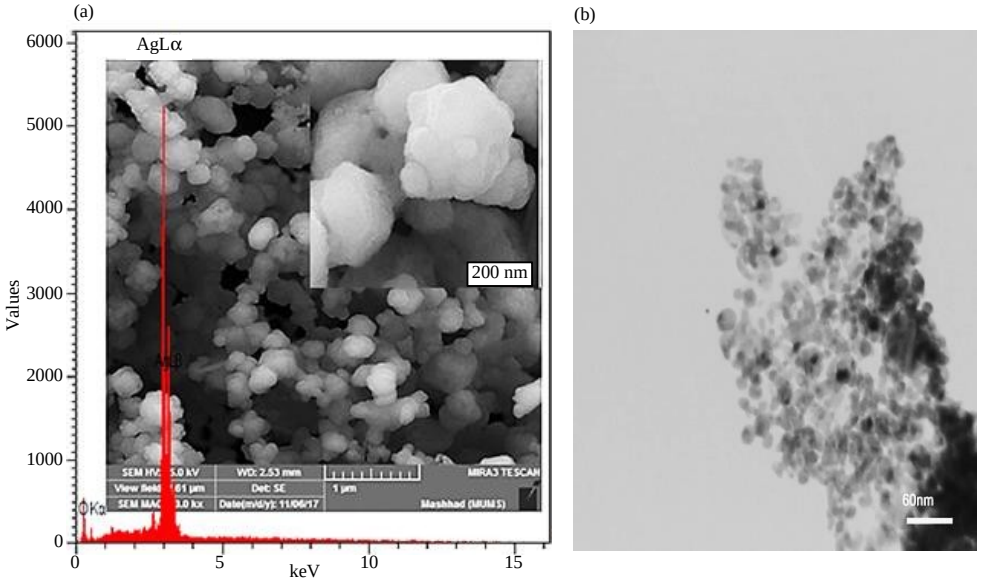

Fig. 6: SEM, TEM and EDS images of Ag_2O NPs electrodeposition in Na_2SO_4 with PVA 10 mL 60 nm, vigorous stirring, (Ag = 95.62 wt.% , O = 4.38 wt.%)

Photodegradation of MG dye by using Ag_2O standard and Ag_2O prepared with calcination at 300°C as catalyst: Ag_2O, a dark brown powder was utilize as a candidate for visible light photocatalyst. Ag_2O is a prospective photocatalyst together dominate superb representation and elevation stabilization, we preparatory a novel utilize of Ag_2O semiconductor which show rapid photîcatalytic behavior to Malachite Green oxalate (MG) with absorption about 617 nm and good stability under visible light (Jiang *et al.*, 2015) through chemical technologies, Promoted Oxidation processes (AOPs) are great used for declination of component, AOPs were based on the generation of highly reactive species such as (•OH) in sufficient value for annihilation organic

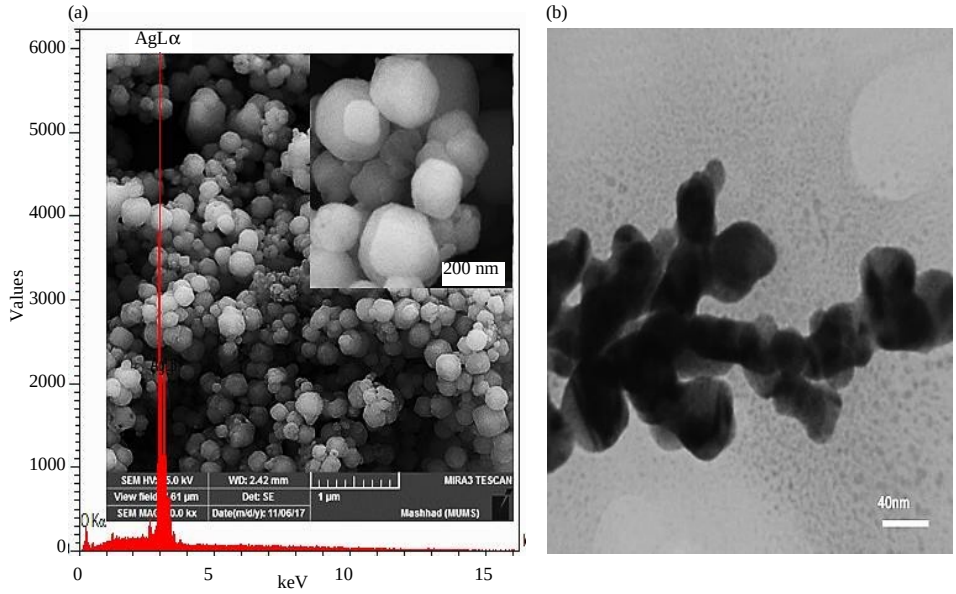

Fig. 7: SEM, TEM and EDS images of Ag_2O NPs electrodeposition in Na_2SO_4 with PVP 10 mL 40 nm, vigorous stirring, (Ag = 94.31 wt.%, O = 5.69 wt.%

pollutants, (•OH) can oxidize a wide domain of pollutants fast and non-selectively (Mohsin *et al*., 2013).

The dye under studying is Malachite Green oxalate (MG) which is specific as a basic dye which is an great water-soluble dye relationship to triphenylmethane family M.wt. 927.01 g/mol (Culp *et al*. 1999; Alderman, 1985; Sawa and Hoten, 2001) and Ag_2O stander 99% are purchased, Fluka , Swiss. photoreactor homemade, supply with lamp-Philips-Holland, mercury (250 W) without glass cover as UV radiation source, UV-Visible spectrophotometer double beam Shimadzu UV 1650 PC Japan, used for decide the declination degree of the (MG) dye solutions. The reactor was consisted of airless To maintain the temperature and electric stirring, hot plate LAB tech. Korea. The lamp's focus vertically above the beaker with space 15 cm. these process occur at 25°C. The suspension pH values were check at required scale using (0.01) N NaOH or (0.01) N HNO_3 solutions were measured via pH meter-Hanna tool, the water mixture was stirred magnetically during the trial, the solution was radiation under ultraviolet light for a specified cycles of time, at several time periods the sample is possessed out by a syringe, later filtered through centrifuge, the centrifuge company ALL-PRO (4000 rpm, 10 min). The floating material was removed by a needle syringe and eject, again at the same speed and for the same length of time. Re-centrifuge for the same period, the absorption of the samples is decided using the UV-V is spectrometer. The rate of color removal and degradation in terms of intensity

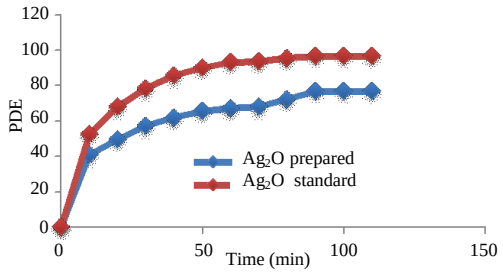

Fig. 8: The degradation efficiency of (MG) absence the UV radiation

change at λ max of dyes was observed by apply the Langmuir Hinshelwood relationship, the activity of decomposition (%) was studied as efficiency (%), after the photoirradiation process, the amount of dye adsorbed and reduced was determined by change in the absorbance of (MG) dye using equation:

$$D\% = \left[\frac{C_0 - C_0}{C_0}\right] \times 100\% \quad (1)$$

Where:

D% = The degradation ratio
C_0 = The initial concentration of dye solution
C_a = The concentration of dyes after adsorption by the catalyst

Dark reaction of Ag_2O catalyst in absence UV radiation: In Dark reaction, test carry out in the without of ultraviolet radiation using Ag_2O as a catalyst. The products were depicted in Fig. 8 in lack ultraviolet radiation no

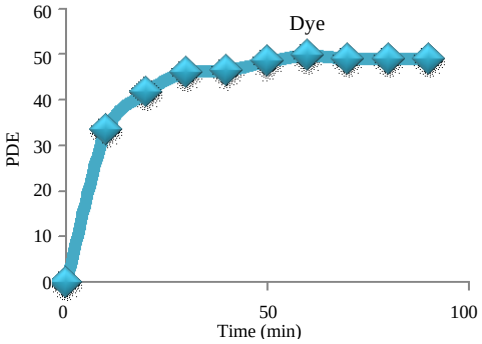

Fig. 9: The photodegradation efficiency of (MG) dyes without the catalyst

deterioration can be observed, slight change in concentration of dye can be show for solution in the dark with catalyst adding, incubation time the first concentrations of dyes is lessen, after a limited period time become fixed due to forming of a monolayer on catalyst surface, the equilibrium occurs after 90 min was calculated decomposition efficiency percentage at 96.722% for the Ag_2O standard, 76.825% for the Ag_2O as-prepared (calcinations at 300°C).

Photodegradation of (MG) dye solution, by UV irradiation in catalyst absence: In photoreaction of (MG) solution, these reaction occur in presence of the UV light with lack of the Ag_2O catalyst. As in Fig. 9, photodegradation efficiency is equal to 49.75% after 90 min of UV treatment with catalyst deprivation.

The influence of Mass catalyst: Mass influence of catalyst onto photocatalytic degradation for (MG) dye**,** solution was scanned under the operation conditions, concentration of dye 4 ppm , intensity of light reached to (250 W), (at 25°C) and variety the amount of Ag_2O for both standard and prepared in range 0.01-0.07 g. The results drawn in Fig. 10a, b), it was be noted the results refer to elevate rate of photocatalytic degradation by excess of the catalyst mass up to top amount and stay constant after that the photocatalytic degradation rate low with the catalyst weight high 0.03 g is the better weight of Ag_2O for both standards and prepared catalyst where photodegradation efficiency is equal to (99.61% Ag_2O standards) and (96.22 % Ag_2O prepared).

The influence of variation in pH in range (2-10) was calculated with maintenance other operation conditions stable at dye concentration of (4) ppm, light power 250 W, Ag_2O catalyst dose 0.03 g at 25°C and variable the pH of dye sol. (Fig. 11a, b).

The influence of pH solution: In this study, the pH effect on degradation of 0.3 g from Ag_2O, depending on (pH_{pzc})

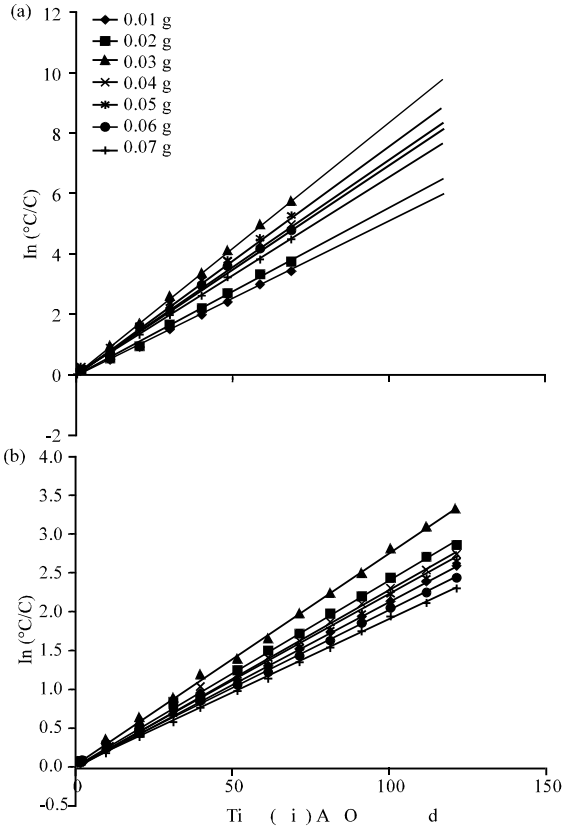

Fig. 10: a) Effect of weight Ag_2O standard on photodegradation efficiency of (MG) and b) Effect of weight Ag_2O prepared on photodegradation efficiency of (MG)

using pH values were adjusts by changing the pH from (2-10). The large degradation was obtained in pH (2) about 99.97% PDE for standard Ag_2O and (99.76 %) PDE for prepared Ag_2O.

The influence of primary dye concentration: The influence of primary dye concentration on the activity of photolysis rate has been studied with Stability of working conditions, light power (250 W), Ag_2O catalyst dose 0.03 g, the pH = (2) at 25°C and the dye concentration is variable in domain (1-7) ppm as in Fig. 12a, b elevated rate of photolysis activity with low initial dye concentration, high adsorption on the catalyst surface with extra dye molecules and negative effect on the interaction between high dye particles with holes or hydroxyl radicals due to the loss of any direct relation for these species (Munesh and Meena, 2012).

Influence of varied temperature: The thermodynamic parameters of the declination of MG was observed. The

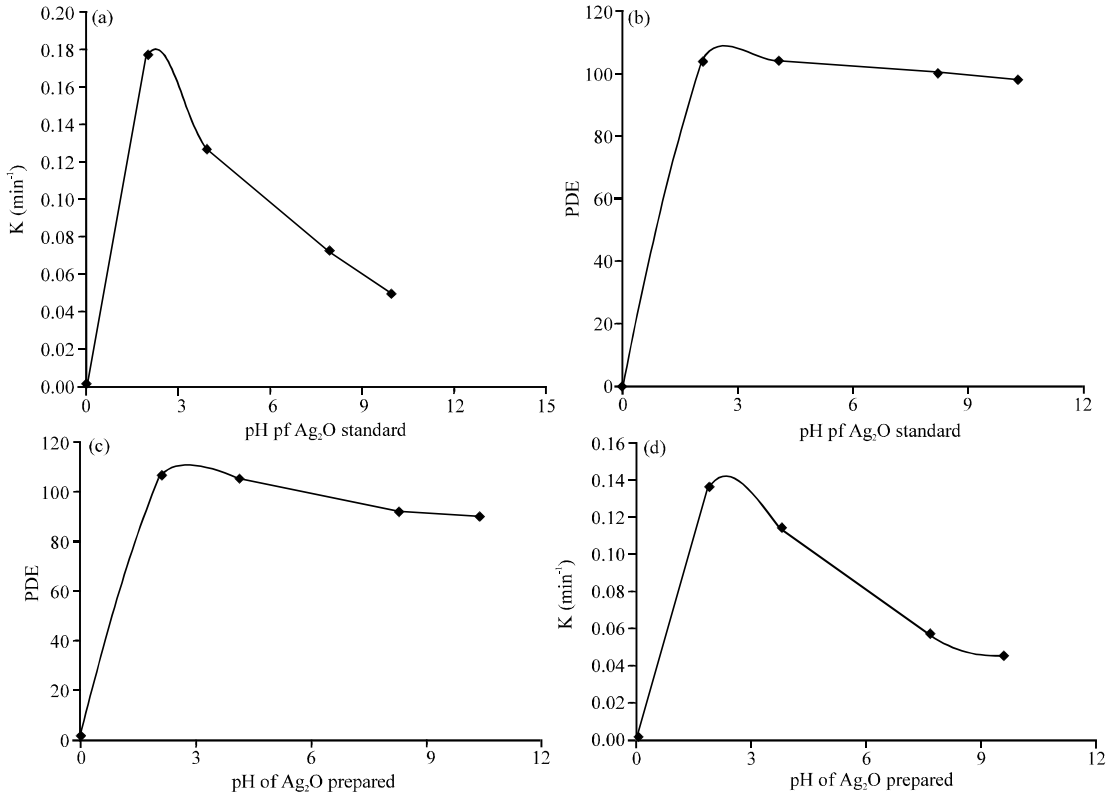

Fig. 11a, b): pH act on photolysis activity of (MG) with 0.03 g Ag_2O Standard and c, d) pH act on photolysis activity of (MG) with 0.03 g Ag_2O prepared

Table 2: AFM measurements of Ag_2O powder electrodeposition of Na_2SO_4 solutions by using PVP, PVA, Glycerin

CSPM imager surface roughness analysis (Amplitude parameters)

Ag_2O	PVP	PVA	Glyserin
Roughness average (Sa) nm	2.8000	4.1400	2.0700
Root mean square (Sq) nm	3.2900	2.6000	2.4200
Surface skewness (Ssk) nm	-0.2290	-0.3040	-0.3130
Surface kurtosis (sku) nm	2.0400	2.5000	1.9600
Sku = (3) mesokurtic, <(3) liptokurtic, > (3) platykurtic	2.5000>	2.0400>	1.9600
Peak-peak (sy) nm	12.8000	11.5000	8.3500
Ten point height (sz) nm	7.2400	11.5000	4.6700
Hybrid parameters			
Mean summit curvature ssc (1/nm)	-1.0000	-0.0166	-1.0000
Root mean square slope (sdq) (1/nm)	0.2640	0.2070	0.2340
Surface area ratio (sdr)	3.2000	2.0000	2.5500
Functional parameters			
Surface bearing index (sbi)	4.9500	2.5200	7.2200
Core fluid retention index (sci)	1.3800	1.3800	1.3000
valley fluid retention index (svi)	0.1030	0.1370	0.1010
Reduced summit height (spk) nm	0.1680	0.8350	0.0000
Core roughness depth (sk) nm	10.2000	7.4800	6.5400
Reduced valley depth (svk) nm	2.2000	3.0800	2.0900
Spatial parameters			
(density of summits) Sds (1/um^2)	0.000	304.0000	0.0000
Fractal dimension	2.390	2.4200	2.5300
Avg. diameter nm	67.650	83.0400	60.8700

(+) ΔH^0 attribute to endothermic interaction, the (+) ΔG^0 result refer to the non-spontaneous interaction in the present research the value of ΔS^0 is negative as in Table 2 and 3 which refer to structure full solvated consisted by dye molecules and intermediate such as hydroxyl radical.

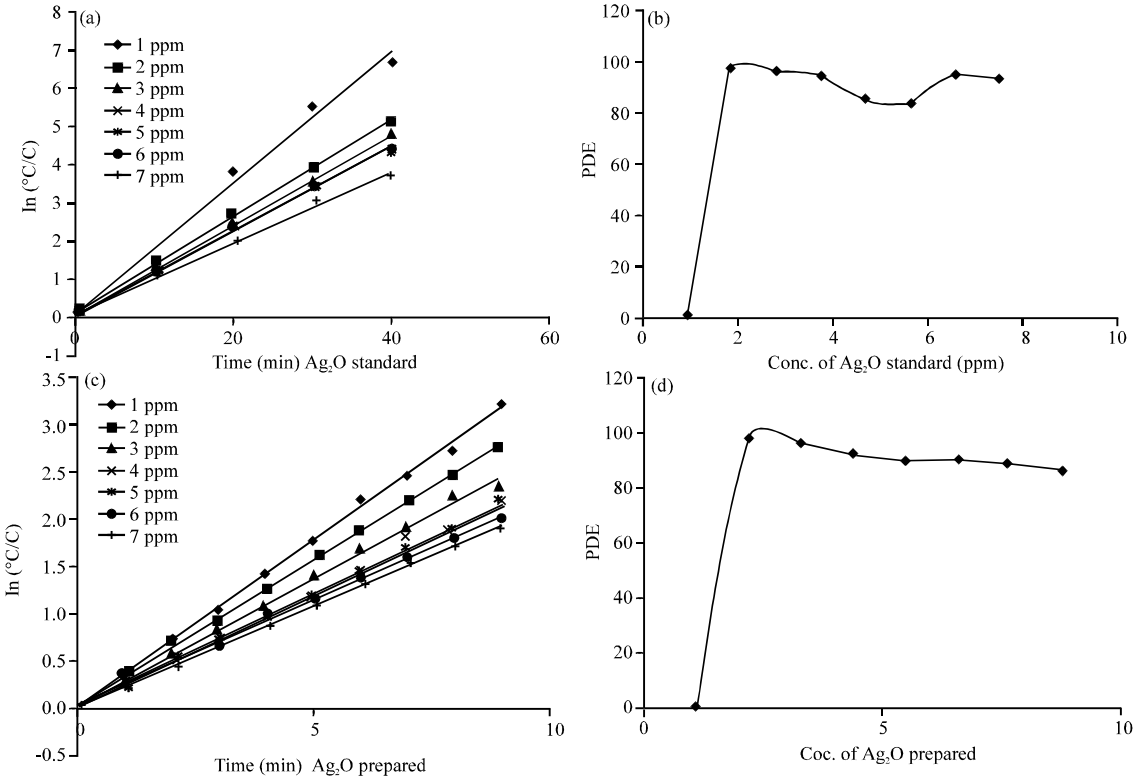

Fig. 12: a, b) The variety in photocatalytic degradation efficiency for MG dye with concentration in presence 0.03 g Ag_2O standard and c, d) The variety in photocatalytic degradation efficiency for MG dye with concentration in presence 0.03 g Ag_2O prepared

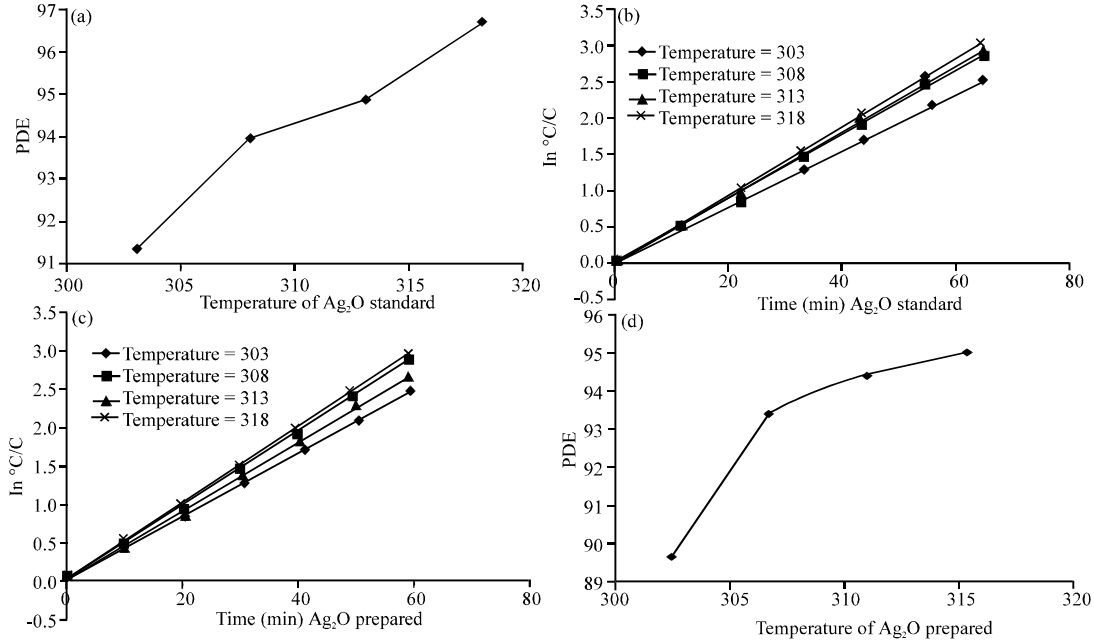

Fig. 13: a, b) The temperature action on photolysis activity of (MG) with 0.03 g Ag_2O stander and c, d) The temperature action on photolysis activity of (MG) with (0.03) g Ag_2O prepared

Table 3: The values of rate constant, thermodynamic and kinetics parameters calculated for photodegradation of (MG) dye at (303-318) K with Ag_2O standard and prepared

		K (sec^{-1})×10^{-5}		ln K		Ea(kJ/mol)		ΔH^0 (kJ/mol)		ΔS^0 (kJ/$mol^{-1}k^{-1}$)		ΔG^0 (kJ/mol)	
T (k°)	1\T	Ag_2O prepared	Ag_2O standard	Ag_2O prepared	Ag_2O standard	Ag_2O prepared	Ag_2O standard	Ag_2O prepared	Ag_2O standard	Ag_2O prepared	Ag_2O standard	Ag_2O prepared	Ag_2O standard
303	0.00330	6.916	6.850	-9.579	-9.588	-	-	3.285	4.431	-	-	95.70	95.634
308	0.00324	7.433	7.516	-9.506	-9.495	-	-	3.243	4.389	-	-	97.20	97.139
313	0.00319	7.716	7.850	-9.469	-9.452	-	-	3.201	4.348	-	-	98.75	98.644
318	0.00314	8.016	8.166	-9.431	-9.412	-	-	3.160	4.306	-	-	100.27	100.149

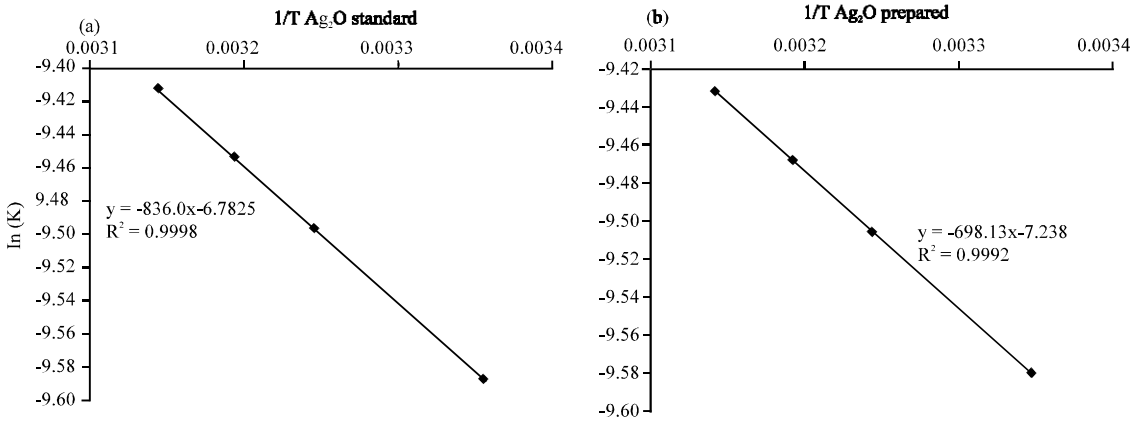

Fig. 14a, b): Arrhenius plot (ln K versus 1/T) of (MG) dye, 0.03 g Ag_2O standard and prepared

CONCLUSION

The silver oxide nanoparticles have been successfully prepared in an electrochemical manner, inexpensive and simple, high precision to control the size and shape of the nanometer scale. To improve the catalytic performance of photolysis and to increase crystallization, the prepared powder was calcination to 300°C. To test the catalytic performance, of prepared silver oxide we compared it with standard silver oxide from fluka, swiss, result refer to (Ea) which was indicated is smaller value (6.950, 5.804) for silver oxide standard and prepared respectively, the thermodynamic parameters of the degradation of MG solutions and silver oxide refer to the positive ΔH^0 certain on endothermic reaction, the positive ΔG^0 result indicate that the non-spontaneous reaction, entropy of activation ΔS^0 is negative, The reactive species such as hydroxyl radical and superoxide anion have been produced from the heterogeneous photocatalytic reaction. The results of the fragmentation of the dye by the catalyst were CO_2 and H_2O.

RECOMMENDATIONS

Future research is the production of low-cost semiconductors capable of eliminating organic pollutants in an easy, simple and controlled manner electrochemical. Cu_2O, TiO_2 as catalysts, low cost and active by using electrochemical approach.

REFERENCES

Alderman, D.J., 1985. Malachite green: A review. J. Fish Dis., 8: 289-298.

Culp, S.J., L.R. Blankenship, D.F. Kusewitt, D.R. Doerge, L.T. Mulligan and F.A. Beland, 1999. Toxicity and metabolism of malachite green and leucomalachite green during short-term feeding to Fischer 344 rats and B6C3F_1 mice. Chemico-Biol. Interact., 122: 153-170.

Fang, C., A.V. Ellis and N.H. Voelcker, 2012. Electrochemical synthesis of silver oxide nanowires, microplatelets and application as SERS substrate precursors. Electrochim. Acta, 59: 346-353.

Gadelmawla, E.S., M.M. Koura, T.M.A. Maksoud, I.M. Elewa and H.H. Soliman, 2002. Roughness parameters. J. Mater. Processing Technol., 123: 133-145.

Ho, J.Y. and M.H. Huang, 2009. Synthesis of submicrometer-sized Cu_2O crystals with morphological evolution from cubic to hexapod structures and their comparative photocatalytic activity. J. Phys. Chem. C., 113: 14159-14164.

Ito, A., M. Shinkai, H. Honda and T. Kobayashi, 2005. Medical application of functionalized magnetic nanoparticles. J. Biosci. Bioeng., 100: 1-11.

Jiang, W., X. Wang, Z. Wu, X. Yue and S. Yuan *et al*., 2015. Silver oxide as superb and stable photocatalyst under visible and near-infrared light irradiation and its photocatalytic mechanism. Ind. Eng. Chem. Res., 54: 832-841.

Kuo, C.H. and M.H. Huang, 2008. Facile synthesis of Cu_2O nanocrystals with systematic shape evolution from cubic to octahedral structures. J. Phys. Chem. C., 112: 18355-18360.

Liao, X.H., J.J. Zhu, X.N. Zhao and H.Y. Chen, 2000. Synthesis of Silver Nanoparticles by electrochemical method. Chem. J. Chin. Univ. Chin., 21: 1837-1839.

Lyu, L.M., W.C. Wang and M.H. Huang, 2010. Synthesis of Ag_2O nanocrystals with systematic shape evolution from cubic to hexapod structures and their surface properties. Chem. A. Eur. J., 16: 14167-14174.

Mohsin, D.H., A.M. Juda and M.S. Mashkour, 2013. Thermodynamic and kinetic study for aromatic rings effect on the photooxidation rate. IJET. IJENS., 13: 34-41.

Munesh, S. and R.C. Meena, 2012. Photocatalytic decolorization of acid red 186 using alternative developed photocatalyst MBIR Dowex 11. Res. J. Chem. Sci., 2: 56-62.

Murray, B.J., Q. Li, J.T. Newberg, E.J. Menke and J.C. Hemminger *et al*., 2005. Shape-and size-selective electrochemical synthesis of dispersed Silver (I) Oxide Colloids. Nano Lett., 5: 2319-2324.

Privett, B.J., S.M. Deupree, C.J. Backlund, K.S. Rao and C.B. Johnson *et al*., 2010. Synergy of nitric oxide and silver sulfadiazine against gram-negative, gram-positive and antibiotic-resistant pathogens. Mol. Pharm., 7: 2289-2296.

Rahman, M.M., A.M. Asiri and S.B. Khan, 2014. Detection of antiemetic drug based on Semiconductor Metal Oxide Nanostructures onto Micro-chips by electrochemical approach. ntl. J. Electrochem. Sci., 9: 6896-6909.

Raposo, M., Q. Ferreira and P.A. Ribeiro, 2007. A guide for atomic force microscopy analysis of soft-condensed matter. Mod. Res. Educ. Top. Microsc., 1: 758-769.

Sagadevan, S., 2016. Synthesis, structural, surface morphology, optical and electrical properties of Silver oxide nanoparticles. Intl. J. Nanoelectron. Mater., 9: 37-49.

Sawa, Y. and M. Hoten, 2001. Antibacterial activity of basic dyes on the dyed acrylic fibers. Sen. I. Gakkaishi, 57: 153-158.

Schoonman, J., 2000. Nanostructured materials in solid state ionics. Solid State Ionics, 135: 5-19.

Yong, N.L., A. Ahmad and A.W. Mohammad, 2013. Synthesis and characterization of silver oxide nanoparticles by a novel method. Int. J. Sci. Eng. Res., 4: 155-158.

Yoshida, A. and N. Toshima, 2014. Gold nanoparticle and gold nanorod embedded PEDOT: PSS thin films as organic thermoelectric materials. J. Electron. Mater., 43: 1492-1497.